Applied Surface Science 317 (2014) 1004–1009

Contents lists available at ScienceDirect

Applied Surface Science

journal homepage: www.elsevier.com/locate/apsusc

Multi- and few-layer graphene on insulating substrate via pulsed laser deposition technique

Indrajeet Kumar, Alika Khare*

Laser and Photonics Lab, Department of Physics, Indian Institute of Technology Guwahati, Guwahati 781039, India

ARTICLE INFO

Article history:
Received 5 April 2014
Received in revised form 24 July 2014
Accepted 31 August 2014
Available online 8 September 2014

Keywords:
Graphene
Pulsed laser deposition
Raman spectroscopy

ABSTRACT

In this paper, multilayer and few layer graphene (FLG) fabricated on fused silica substrate by pulsed laser deposition (PLD) technique without using any catalyst is reported. The effect of deposition temperature onto the formation of graphene layers is investigated. Raman spectra showed the characteristic features of sp^2 bonded carbon atoms; G band, D band and 2D band. The line shape of 2D band structure and the relative intensities of G and 2D bands were used to estimate the number of graphene layers. The graphene layers deposited via PLD at room temperature has I_{2D}/I_G ratio ~0.33, confirming the formation of multilayer whereas that of deposited at substrate temperature 700 °C is ~0.47 confirming the formation of less than five layers of graphene; few layers graphene. The decrease in separation of subpeaks of 2D band with deposition temperature further confirms the reduction in the number of layers of graphene from ~10 deposited at room temperature to less than 5 layers at that of 700 °C. The surface morphology of the deposited samples was recorded by field emission scanning electron microscope and transmission electron microscope.

1. Introduction

Graphene is a thermodynamically stable two-dimensional hexagonal lattice structure of sp^2 bonded carbon atoms and considered as the building block for carbon allotropes of all other dimensionality; a stack of graphene layers and wrapped graphene layers forms graphite and carbon nanotubes, respectively while topological defects in them forms fullerenes. It possesses exceptional thermal, electrical, optical and mechanical properties leading to its potential applications in research and industry as transparent electrodes, field emitters, biosensors, etc. [1–8]. Graphene has been prepared by several techniques viz.; chemical vapor deposition (CVD), pulsed laser deposition (PLD), chemical synthesis, micromechanical cleavage, etc. [9–15]. The first experimentally produced graphene was obtained in 2004 by mechanical exfoliation of graphite [16]. Graphene was also obtained by heating silicon carbide to high temperatures (>1100 °C) [17,18]. A very promising method to produce mono-layer graphene is chemical vapor deposition (CVD) on metal surfaces [9,19]. In most of the cases, either graphene is deposited onto metal substrates and then transferred to other substrates for further studies or using a precursor. During the process of transferring graphene layers, there is a possibility to induce defects in it. Use of a precursor may also induce defects in graphene sheets. Among all the techniques, PLD technique offers the advantage to grow the graphene layers directly onto any substrate [20–22]. In PLD technique, deposited species (laser ablated particles/ions) are of high kinetic energy therefore good quality thin films can be deposited at relatively lower temperature compared to that of the other techniques. The fabrication of graphene using PLD technique was reported by Zhang et al. in the substrate temperature range of 1100–1300 °C using excimer laser onto Ni substrate [21]. Graphene can be characterized by micro-Raman as it is highly sensitive towards sp^2 bonded carbon atoms by exciting it with a laser in the visible range [23,24]. The presence of disorder in carbon system; from graphite to carbon nanotubes, can be investigated and quantified using Raman spectrum. In case of graphene, the number of atomic layers can be clearly estimated by micro-Raman spectrum. The Raman signature of graphene has two most intense peaks at ~1585 cm^{-1} (G band) and another one at ~2730 cm^{-1} (2D band). The presence of disorder in graphene brings two more Raman features other than G and 2D band, these are at ~1350 cm^{-1} (D band) and ~1620 cm^{-1} (D′ band) originated from intervalley and intravalley defect induced resonant scattering processes [25].

In the present paper, the evolution of graphene from multilayer to few layers onto the fused silica substrate as a function of deposition temperature by pulsed laser ablation of graphite target without using any catalyst is reported. Multilayer graphene (MLG) and few

* Corresponding author. Tel.: +91 03612582705; fax: +91 3612582749.
E-mail address: alika@iitg.ernet.in (A. Khare).

http://dx.doi.org/10.1016/j.apsusc.2014.08.185
0169-4332/

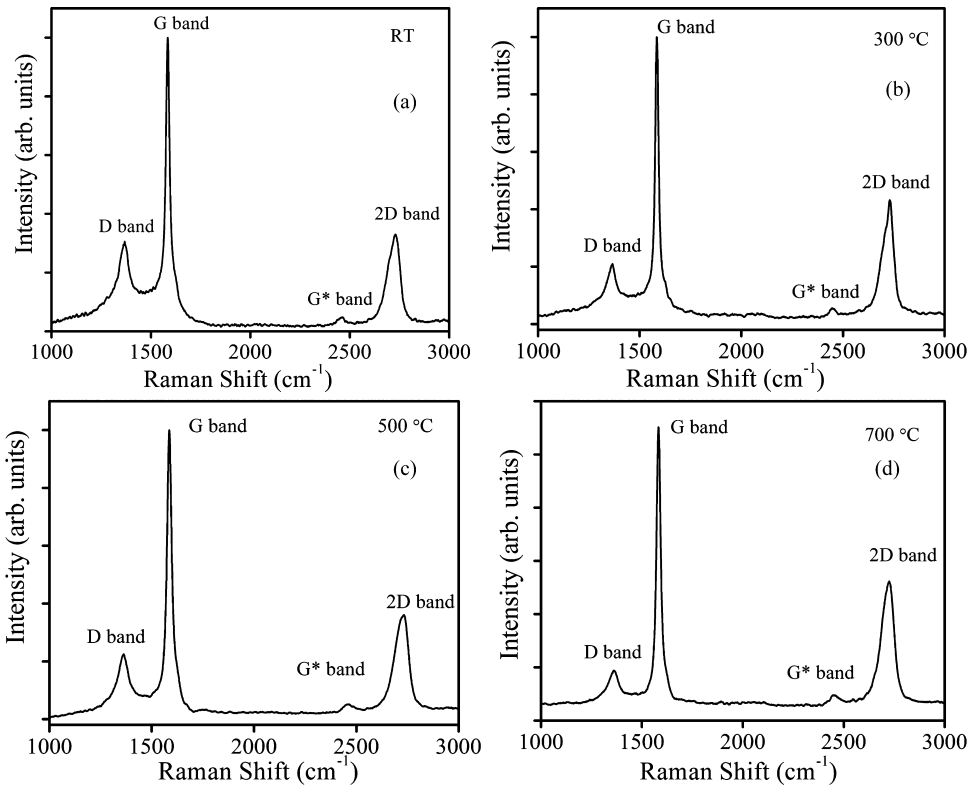

Fig. 1. Raman spectrum of graphene layers deposited at substrate temperature (a) RT, (b) 300 °C, (c) 500 °C and (d) 700 °C.

layer graphene (FLG) were characterized by Raman spectrometer, transmission electron microscope (TEM) and field emission scanning electron microscope (FESEM).

2. Experimental details

The graphene samples were prepared by PLD technique at various substrate temperatures. The graphite target was ablated by focusing the second harmonic of high power *Q*-switched Nd:YAG laser (Quanta Ray INDI-HG) in oxygen ambient and deposited onto the fused silica substrates. The laser fluence was kept at ~5 J/cm^{-2}. The substrate to graphite target distance was maintained at 3 cm for all the samples. The graphite target was rotated continuously in order to expose the fresh surface for each laser shot during the deposition process. The ablation chamber was initially evacuated at base pressure of ~10^{-6} mbar and then maintained at 0.1 mbar of oxygen while depositing graphene layers. The graphene layers were deposited for 15 min at room temperature (RT) to 700 °C.

The Raman spectra of graphene layers were recorded with the micro-Raman setup (Horiba Jobin Vyon, LabRam HR 800) using three different laser excitation sources: 488 nm, 514 nm and 633 nm in a back scattering geometry, at room temperature. FESEM (Zeiss, Sigma) and TEM (JEOL, JEM 2100) images were recorded to study the surface morphology and selected area electron diffraction (SAED) pattern of the graphene layers.

3. Results and discussion

The Raman spectra for excitation laser source at 514 nm of the multilayer graphene deposited on fused silica substrate at (a) RT, (b) 300 °C, (c) 500 °C and (d) 700 °C are shown in Fig. 1. The main Raman scattering features of graphitic materials at 1367 cm^{-1} (D band), 1584 cm^{-1} (G band) and 2730 cm^{-1} (2D band) are clearly observed. The Raman D band arises due to the presence of disorder in graphene and depends on the breathing mode of the aromatic rings. The disorder may be due to stacking between two layers, atomic defects within the layer and edges in finite crystallite sites [26,27]. The G band originates from first order Raman scattering process and corresponds to the in-plane vibration of sp^2 bonded carbon atoms [28]. The FWHM of the G band is 24.8 cm^{-1} for the graphene layers deposited at RT and decreased to 21.7 cm^{-1} for that of deposited at 700 °C. The narrowing in the FWHM of G band at higher substrate temperature indicates the increase in crystallinity in graphene layers deposited at 700 °C. The intensity ratio of D and G bands (I_D/I_G) for graphene layers deposited at different substrate temperature is listed in Table 1. The intensity ratio I_D/I_G of graphene layers was observed to decrease with the increase in substrate temperature. The decrease in D band intensity and hence the intensity ratio, I_D/I_G, with the increasing substrate temperature indicates the decrease in defect and hence formation of ordered graphene layers at higher substrate temperature.

The 2D band observed at 2730 cm^{-1} originates from a two phonon double resonance Raman process and is closely related to

Table 1
Raman intensity ratio I_D/I_G of graphene layers as a function of substrate temperature.

Deposition temperature	RT	100 °C	200 °C	300 °C	400 °C	500 °C	600 °C	700 °C
I_D/I_G	0.31	0.36	0.27	0.22	0.22	0.21	0.16	0.13

the band structure of the graphene layers [29]. The splitting of 2D band and the relative intensities of 2D and G band (I_{2D}/I_G) is indicative of number of layers in the graphene samples [30,31]. Fig. 2 illustrates the enlarged 2D band shape along with multiple peak fitting of graphene layers deposited at (a) RT, (b) 300 °C, (c) 500 °C and (d) 700 °C. The Raman 2D band was de-convoluted into subpeaks using Lorentzian lineshape. The intensity ratio, I_{2D}/I_G, the number of subpeaks of 2D band and the peak separation between them is sensitive to the number of graphene layers [32]. The 2D band shape and intensity ratio I_{2D}/I_G in Raman spectra shows multilayer graphene (MLG) formation at RT. The I_{2D}/I_G ratio of MLG was ~0.33 and increased with increasing substrate temperature. At substrate temperature of 700 °C, the I_{2D}/I_G ratio of FLG became ~0.47 which corresponds to less than 5 layers [33]. For monolayer graphene, the 2D band has single Lorentzian peak, whereas bilayer graphene has four Lorentzian subpeaks. Here only two subpeaks were observed for all the samples confirming that number of graphene layers is more than two. The wavenumber separation of two subpeaks was measured to estimate the number of graphene layers. For the MLG, deposited at RT, the separation between two subpeaks in 2D band was 32.25 cm^{-1} indicating the presence of ~10 layers. The wavenumber separation was found to decrease with increase in substrate temperature, indicating the decrease in number of graphene layers with increase in substrate temperature. At substrate temperature of 700 °C, the wavenumber separation was found to be 28.21 cm^{-1} between two subpeaks for the FLG, clearly indicating the presence of approximately 4–5 layers [22]. In addition to these bands, a broad band was observed at 2459 cm^{-1} (G* band) in all the samples, which was absent in that of the graphite target used for the PLD. The Raman G* band originates from double resonance Raman scattering, a combination of the zone boundary in-plane longitudinal acoustic (iLA) phonon and the in-plane transverse optical (iTO) phonon modes [34]. The differences in the Raman spectra of these samples, deposited at various substrate temperatures, can be explained by the dependence of the diffusion coefficient on the deposition temperatures. At RT and low substrate temperatures, the carbon atoms with a certain amount of energy are deposited onto the fused silica substrate in highly localized manner due to the lack of sufficient mobility to form crystalline structure. As substrate temperature increases, the mobility of the carbon adatoms increases due to increase in the diffusion coefficient, which is given by Eq. (1) [33].

$$D = D_0 \exp\left(-\frac{E_a}{RT}\right) \quad (1)$$

where D is the diffusion coefficient, D_0 is the maximum diffusion coefficient (at infinite temperature), E_a is the activation energy for diffusion, T is the substrate temperature and R is the gas constant. As the rate of diffusion increases at higher temperature, adatoms rearrange themselves to form more ordered graphene layers, which were reflected by the lower intensity ratio I_D/I_G in the Raman spectrum with the increasing substrate temperature (Table 1). After deposition, the cooling rate was kept same for all the samples deposited at 300 °C, 500 °C and 700 °C. The samples were allowed to cool at the rate of ~3.3 °C/min up to 100 °C and then left for natural cooling. The ambient pressure of the chamber was maintained at deposition pressure (0.1 mbar of O_2 gas) during the cooling process. The slower cooling rate provides the sufficient time for the adatoms to rearrange themselves. At the elevated substrate temperature of 700 °C, the mobility of the carbon atoms was high enough and they had sufficient time to diffuse due to slow cooling rate, and hence formed FLG. It agrees well to the 2D band shape of Raman spectrum of FLG as shown in Fig. 2.

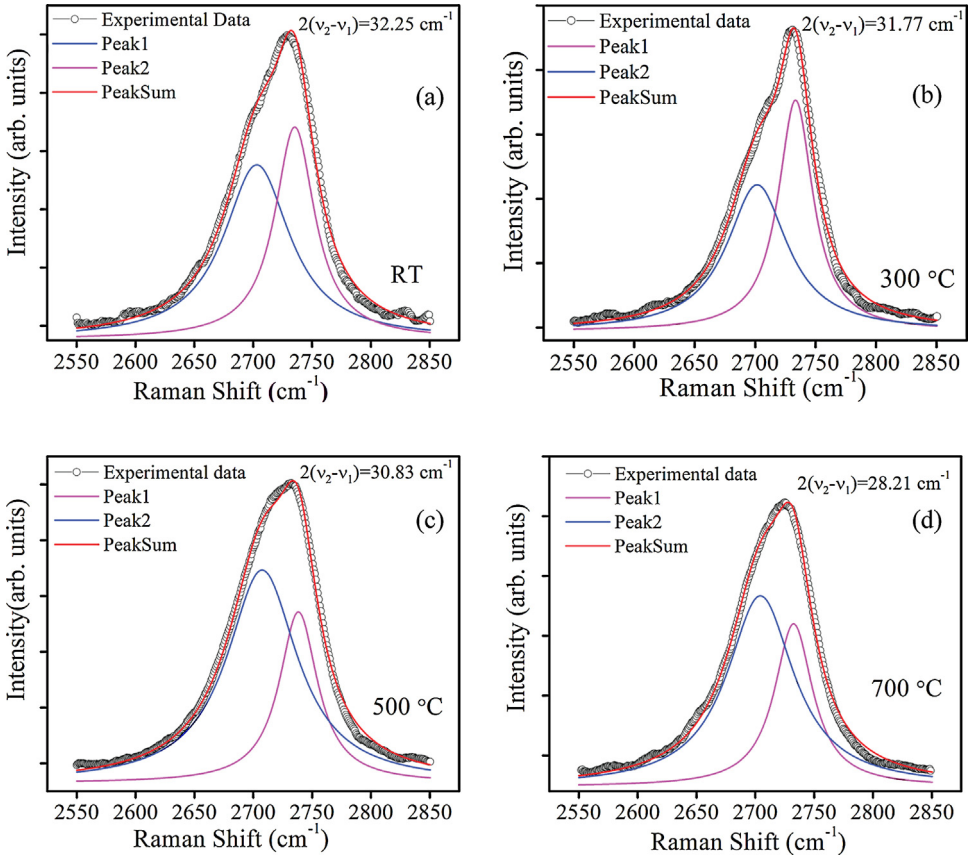

Fig. 2. 2D band splitting of graphene layers deposited at substrate temperature (a) RT, (b) 300 °C, (c) 500 °C and (d) 700 °C.

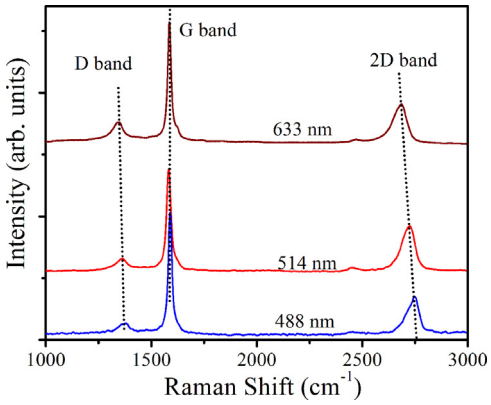

Fig. 3. Variation in Raman spectrum of graphene sample prepared at 700 °C with excitation laser wavelength.

Table 2
Dispersion of D and 2D band with the excitation laser energy in Raman spectra of FLG.

Excitation wavelength	D band	G band	G* band	2D band
488 nm	1377 cm^{-1}	1586 cm^{-1}	2452 cm^{-1}	2747 cm^{-1}
514 nm	1367 cm^{-1}	1584 cm^{-1}	2459 cm^{-1}	2730 cm^{-1}
633 nm	1344 cm^{-1}	1583 cm^{-1}	2472 cm^{-1}	2684 cm^{-1}

Fig. 3 shows the dependence of Raman spectra of Graphene layers (deposited at 700 °C) on the excitation laser wavelength. The position of G band is nearly independent of the excitation laser wavelength. All the other bands of graphene layers; D, 2D and G* shows the linear dispersion behavior due to double resonance [35]. By changing the laser excitation energy, different points in momentum space for the electronic and phonon dispersion are probed [36]. The Raman shift position of D, 2D, G and G* band at different laser photon energy are tabulated in Table 2. The Raman shift of D and 2D band increases with the laser photon energy. The plot of D and 2D position as a function of laser photon energy is shown in Fig. 4.

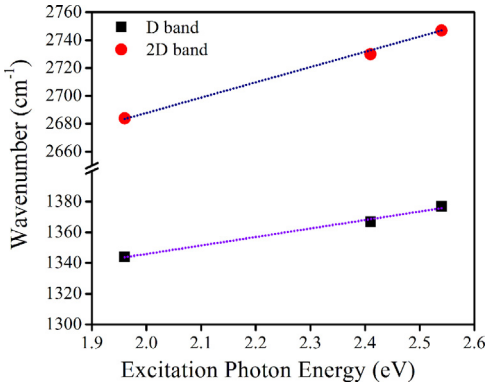

Fig. 4. Dispersion of D and 2D peak position of FLG.

The slopes $\partial\bar{\nu}/\partial E_1$ for D and 2D band were calculated from the linear fitting of the $\bar{\nu}$ versus E_l graph. The slope $\partial\bar{\nu}_{2D}/\partial E_1$ is approximately twice of the slope $\partial\bar{\nu}_D/\partial E_1$ which confirm that 2D band is the second harmonic of the D band.

$$\frac{\partial\bar{\nu}_D}{\partial E_l} = 55.3 \ \ cm^{-1}/eV \tag{2}$$

$$\frac{\partial\bar{\nu}_{2D}}{\partial E_l} = 109.5 \ \ cm^{-1}/eV \tag{3}$$

The Raman G* band of FLG also showed dispersive behavior. The acoustic (LA) phonon associated with G* band has less contribution to the intense singularity in the double resonance phonon density of states. As a result, it is weaker and less pronounced compared to that of D and 2D bands. Its Raman shift decreases with the increase in laser photon energy [26,35].

Fig. 5 shows the TEM image and corresponding SAED pattern of multilayer graphene deposited at RT. The graphene layers shown in TEM micrograph, Fig. 5(a) and (b), are randomly oriented which is also reflected in its SAED pattern with overlapping diffraction points in Fig. 5(c). Fig. 6(a) shows the TEM image of few layers

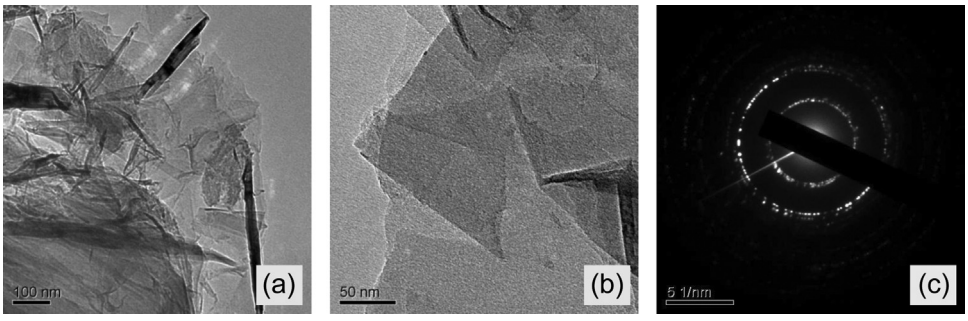

Fig. 5. (a), (b) TEM images and (c) SAED pattern of graphene sample prepared at RT.

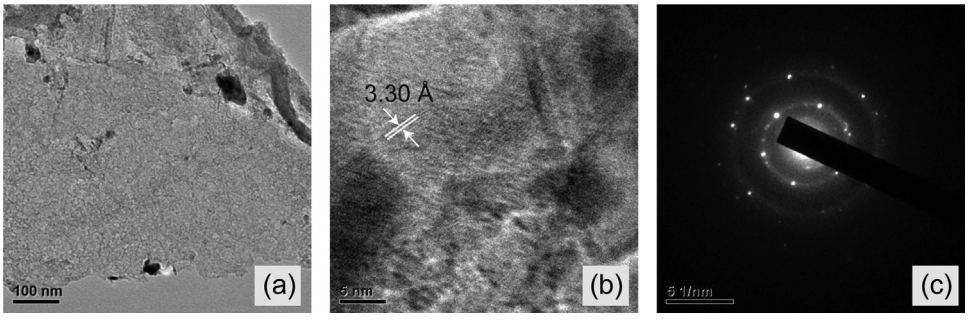

Fig. 6. (a) TEM images, (b) HRTEM and (c) SAED pattern of graphene sample prepared at 700 °C.

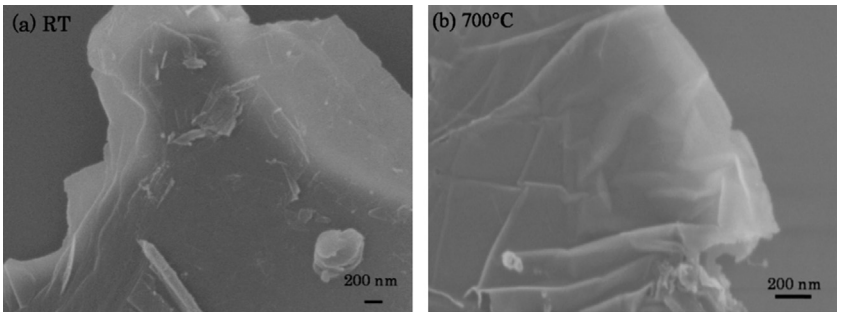

Fig. 7. FESEM image of graphene layers deposited at (a) RT and (b) 700 °C.

graphene deposited at substrate temperature of 700 °C. The corresponding high-resolution TEM (HRTEM) image is shown in Fig. 6(b). To identify the crystallinity of graphene, SAED pattern was recorded from corresponding domain. As shown in Fig. 6(c), spots in diffraction pattern were in hexagonal geometry, confirming that the FLG formed at 700 °C has high crystallinity. The lattice d-spacing were calculated from HRTEM image, Fig. 6(b), and SAED pattern, Fig. 6(c), using Gatan Digital Micrograph software attached with the TEM instrument and found to be ~3.30 Å. The interlayer spacing value is closely related to its theoretical value 3.35 Å (crystalline graphite), confirming the good stacking of graphene layers. These TEM results support well the observation made in Raman spectra discussed above and again confirming that prepared sample are MLG and FLG at deposition temperature of RT and 700 °C, respectively.

Fig. 7 shows the FESEM image of graphene layers prepared at RT and 700 °C. From color contrast of the images, it can be easily seen that the number of graphene layers are less at higher substrate temperature with less defect, which is again in accordance with the Raman spectrum.

4. Conclusion

Graphene layers were prepared via PLD technique at different substrate temperatures from RT to 700 °C without using any catalyst in single step. 4–5 graphene layers were formed at 700 °C whereas MLG were formed at lower substrate temperature. Raman spectra showed the D, G, 2D and G* bands of sp^2 carbon networks. The decrease in I_D/I_G ratio with the increase in substrate temperature indicated the reduction of defects at higher temperature. The presence of G* band and the splitting of 2D band confirmed the formation of multilayer and few layer graphene. The sample deposited at 700 °C indicates the formation of few layers of graphene compared to that of deposited at RT due to the diffusion of the adatoms of carbon at elevated substrate temperature. TEM images showed the formation of folded and disordered graphene in random orientation at RT whereas few layer graphene with high crystallinity were formed at 700 °C.

Acknowledgement

The TEM, FESEM and Laser Raman facility of CIF, IIT Guwahati is acknowledged.

References

[1] M.J. Allen, V.C. Tung, R.B. Kaner, Honeycomb carbon: a review of graphene, Chem. Rev. 110 (2010) 132–145.
[2] R. Prasher, Graphene spreads the heat, Science 328 (2010) 185–186.
[3] A.K. Geim, K.S. Novoselov, The rise of graphene, Nat. Mater. 6 (2007) 183–191.
[4] F. Bonaccorso, Z. Sun, T. Hasan, A.C. Ferrari, Graphene photonics and optoelectronics, Nat. Photonics 4 (2010) 611–622.
[5] C. Lee, X. Wei, J.W. Kysar, J. Hone, Measurement of the elastic properties and intrinsic strength of monolayer graphene, Science 321 (2008) 385–388.
[6] M.S. Lee, K. Lee, S.Y. Kim, H. Lee, J. Park, K.H. Choi, H.K. Kim, D.G. Kim, D.Y. Lee, S. Nam, J.U. Park, High-performance, transparent, and stretchable electrodes using graphene–metal nanowire hybrid structures, Nano Lett. 13 (2013) 2814–2821.
[7] Y.D. Kim, M.H. Bae, J.T. Seo, Y.S. Kim, H. Kim, J.H. Lee, J.R. Ahn, S.W. Lee, S.H. Chun, Y.D. Park, Focused-laser-enabled p–n junctions in graphene field-effect transistors, ACS Nano 7 (2013) 5850–5857.
[8] T. Kuila, S. Bose, P. Khanra, A.K. Mishra, N.H. Kim, J.H. Lee, Recent advances in graphene-based biosensors, Biosens. Bioelectron. 26 (2011) 4637–4648.
[9] K.S. Kim, Y. Zhao, H. Jang, S.Y. Lee, J.M. Kim, K.S. Kim, J.H. Ahn, P. Kim, J.Y. Choi, B.H. Hong, Large-scale pattern growth of graphene films for stretchable transparent electrodes, Nature 457 (2009) 706–710.
[10] K. Wang, G. Tai, K.H. Wong, S.P. Lau, W. Guo, Ni induced few-layer graphene growth at low temperature by pulsed laser deposition, AIP Adv. 1 (2011) 022141.
[11] S. Stankovich, D.A. Dikin, R.D. Piner, K.A. Kohlhaas, A. Kleinhammes, Y. Jia, Y. Wu, S.T. Nguyen, R.S. Ruoff, Synthesis of graphene-based nanosheets via chemical reduction of exfoliated graphite oxide, Carbon 45 (2007) 1558–1565.
[12] P. Blake, E.W. Hill, A.H.C. Neto, K.S. Novoselov, D. Jiang, R. Yang, T.J. Booth, A.K. Geim, Making graphene visible, Appl. Phys. Lett. 91 (2007) 063124.
[13] T.N. Lambert, C.C. Luhrs, C.A. Chavez, S. Wakeland, M.T. Brumbach, T.M. Alam, Graphite oxide as a precursor for the synthesis of disordered graphenes using the aerosol-through-plasma method, Carbon 48 (2010) 4081–4089.
[14] E. Tatarova, J. Henriques, C.C. Luhrs, A. Dias, J. Phillips, M.V. Abrashev, C.M. Ferreira, Microwave plasma based single step method for free standing graphene synthesis at atmospheric conditions, Appl. Phys. Lett. 103 (2013) 134101.
[15] B. Shen, J. Ding, X. Yan, W. Feng, J. Li, Q. Xue, Influence of different buffer gases on synthesis of few-layered graphene by arc discharge method, Appl. Surf. Sci. 258 (2012) 4523–4531.
[16] K.S. Novoselov, A.K. Geim, S.V. Morozov, D. Jiang, Y. Zhang, S.V. Dubonos, I.V. Grigorieva, A.A. Firsov, Electric field effect in atomically thin carbon films, Science 306 (2004) 666–669.
[17] K.V. Emtsev, A. Bostwick, K. Horn, J. Jobst, G.L. Kellogg, L. Ley, J.L. McChesney, T. Ohta, S.A. Reshanov, J. Röhrl, E. Rotenberg, A.K. Schmid, D. Waldmann, H.B. Weber, T. Seyller, Towards wafer-size graphene layers by atmospheric pressure graphitization of silicon carbide, Nat. Mater. 8 (2009) 203–207.
[18] J. Hass, R. Feng, T. Li, X. Li, Z. Zong, W.A. de Heer, P.N. First, E.H. Conrad, C.A. Jeffrey, C. Berger, Highly ordered graphene for two dimensional electronics, Appl. Phys. Lett. 89 (2006) 143106.
[19] A. Reina, X. Jia, J. Ho, D. Nezich, H. Son, V. Bulovic, M.S. Dresselhaus, J. Kong, Large area, few-layer graphene films on arbitrary substrates by chemical vapor deposition, Nano Lett. 9 (2009) 30–35.
[20] M. Qian, Y.S. Zhou, Y. Gao, J.B. Park, T. Feng, S.M. Huang, Z. Sun, L. Jiang, Y.F. Lu, Formation of graphene sheets through laser exfoliation of highly ordered pyrolytic graphite, Appl. Phys. Lett. 98 (2011) 173108.
[21] H. Zhang, P.X. Feng, Fabrication and characterization of few-layer graphene, Carbon 48 (2010) 359–364.
[22] A.T.T. Koh, Y.M. Foong, D.H.C. Chua, Cooling rate and energy dependence of pulsed laser fabricated graphene on nickel at reduced temperature, Appl. Phys. Lett. 97 (2010) 114102.
[23] A.C. Ferrari, Raman spectroscopy of graphene and graphite: disorder, electron-phonon coupling, doping and nonadiabatic effects, Solid State Commun. 143 (2007) 47–57.
[24] A.C. Ferrari, D.M. Basko, Raman spectroscopy as a versatile tool for studying the properties of graphene, Nat. Nanotechnol. 8 (2013) 235–246.
[25] E.H. Martins Ferreira, M.V.O. Moutinho, F. Stavale, M.M. Lucchese, R.B. Capaz, C.A. Achete, A. Jorio, Evolution of the Raman spectra from single-, few-, and many-layer graphene with increasing disorder, Phys. Rev. B 82 (2010) 125429.
[26] J. Maultzsch, S. Reich, C. Thomsen, Double-resonant Raman scattering in graphite: interference effects, selection rules, and phonon dispersion, Phys. Rev. B 70 (2004) 155403.
[27] P. Vancsó, G.I. Márk, P. Lambin, A. Mayer, C. Hwang, L.P. Biró, Effect of the disorder in graphene grain boundaries: a wave packet dynamics study, Appl. Surf. Sci. 291 (2014) 58–63.

[28] F. Tuinstra, J.L. Koenig, Raman spectrum of graphite, J. Chem. Phys. 53 (1970) 1126–1130.
[29] L.M. Malard, M.A. Pimenta, G. Dresselhaus, M.S. Dresselhaus, Raman spectroscopy in graphene, Phys. Rep. 473 (2009) 51–87.
[30] A.C. Ferrari, J.C. Meyer, V. Scardaci, C. Casiraghi, M. Lazzeri, F. Mauri, S. Piscanec, D. Jiang, K.S. Novoselov, S. Roth, A.K. Geim, Raman spectrum of graphene and graphene layers, Phys. Rev. Lett. 97 (2006) 187401.
[31] Z. Ni, Y. Wang, T. Yu, Z. Shen, Raman spectroscopy and imaging of graphene, Nano Res. 1 (2008) 273–291.
[32] L.Y. Lin, D.E. Kim, W.K. Kim, S.C. Jun, Friction and wear characteristics of multi-layer graphene films investigated by atomic force microscopy, Surf. Coat. Technol. 205 (2011) 4864–4869.
[33] A.T.T. Koh, Y.M. Foong, D.H.C. Chua, Comparison of the mechanism of low defect few-layer graphene fabricated on different metals by pulsed laser deposition, Diam. Relat. Mater. 25 (2012) 98–102.
[34] D. Yoon, H. Moon, H. Cheong, J.S. Choi, J. Ae Choi, B. Ho Park, Variations in the Raman spectrum as a function of the number of graphene layers, J. Korean Phys. Soc. 55 (2009) 1299–1303.
[35] D.L. Mafra, G. Samsonidze, L.M. Malard, D.C. Elias, J.C. Brant, F. Plentz, E.S. Alves, M.A. Pimenta, Determination of LA and TO phonon dispersion relations of graphene near the Dirac point by double resonance Raman scattering, Phys. Rev. B 76 (2007) 233407.
[36] M.A. Pimenta, G. Dresselhaus, M.S. Dresselhaus, L.G. Cancado, A. Jorio, R. Saito, Studying disorder in graphite-based systems by Raman spectroscopy, Phys. Chem. Chem. Phys. 9 (2007) 1276–1291.